

ILASH: A Predictive Neural Architecture Search Framework for Multi-Task Applications

*Md Hafizur Rahman, †Md Mashfiq Rizvee, †Sumaiya Shomaji and *Prabuddha Chakraborty

*Department of Electrical and Computer Engineering, University of Maine

† Department of Electrical Engineering and Computer Science, University of Kansas

Abstract—Artificial intelligence (AI) is widely used in various fields including healthcare, autonomous vehicles, robotics, traffic monitoring, and agriculture. Many modern AI applications in these fields are multi-tasking in nature (i.e. perform multiple analysis on same data) and are deployed on resource-constrained edge devices requiring the AI models to be efficient across different metrics such as power, frame rate, and size. For these specific use-cases, in this work, we propose a new paradigm of neural network architecture (ILASH) that leverages a layer sharing concept for minimizing power utilization, increasing frame rate, and reducing model size. Additionally, we propose a novel neural network architecture search framework (ILASH-NAS) for efficient construction of these neural network models for a given set of tasks and device constraints. The proposed NAS framework utilizes a data-driven intelligent approach to make the search efficient in terms of energy, time, and CO₂ emission. We perform extensive evaluations of the proposed layer shared architecture paradigm (ILASH) and the ILASH-NAS framework using four open-source datasets (UTKFace, MTF, CelebA, and Taskonomy). We compare ILASH-NAS with AutoKeras and observe significant improvement in terms of both the generated model performance and neural search efficiency with up to 16x less energy utilization, CO₂ emission, and training/search time.

Index Terms—Neural Architecture Search (NAS), Deep Learning, Multitask Learning.

I. INTRODUCTION

ARTIFICIAL intelligence (AI) is a rapidly growing market estimated to surpass 1 Trillion USD by 2027 [1]. AI is being used in most modern applications, devices, and services across almost all domains including automotive [2]–[4], digital manufacturing [5], [6], healthcare [7]–[9], and retail [10], [11]. However, one of the major concerns with AI, that can potentially slow down its growth, is rooted in the energy utilization and carbon emission aspects. In [12], researchers conducted a life cycle assessment on the training of various prevalent large AI models. The results indicated that this process could release over 626,000 pounds of carbon dioxide equivalent to almost five times the cumulative emissions of an average American car throughout its entire lifespan (including manufacturing). The two main sources of energy utilization and carbon emission are:

- 1) **Neural Architecture Search (NAS) & Training:** The automated NAS process can be extremely power-hungry. In certain cases, energy utilization can reach up to 4.98×10^2 kWh-PUE and carbon emission can exceed 4.75×10^2 lbs for just obtaining one AI model (see Table I).
- 2) **Inferencing:** AI models being used in billions of IoT edge devices (for inferencing tasks) also lead to a large

amount of cumulative energy consumption and carbon emission. The “*State of IoT—Spring 2023*” report shows a total of 14.3 billion active IoT endpoints [13].

In this work, we propose to minimize both of these avenues of energy expenditure and CO₂ emission by developing an Intelligent LAYER SHARED (ILASH) neural architecture paradigm and an associated neural architecture search algorithm that leverages AI for efficiency. ILASH models reduce energy utilization and CO₂ emission by sharing intermediate computation outcomes (layer-outputs) across different tasks (layer-sharing) while the proposed AI-Guided NAS (ILASH-NAS) makes building these ILASH models highly energy efficient. Our proposed ILASH architecture, the methodology of layer sharing, and the AI-guided neural architecture search process (for building ILASH networks) are novel compared to existing works. We use ILASH-NAS to search models for different multi-task applications using standard datasets such as UTKFace [14], MTF [15], CelebA [16], and Taskonomy [17] with Raspberry Pi 4 Model B, Jetson Orin Nano, Jetson Nano, and Jetson AGX nano as target edge devices. We observe up to 16x reduction in energy utilization and CO₂ emission during the neural architecture search and training process compared to state-of-the-art multi-task NAS algorithms (AutoKeras). The layer-sharing aspect of the final model also led to 3x reduction in inferencing energy and CO₂ emission compared to state-of-the-art counterparts. In this article, we make the following research contributions:

- 1) Designed a novel class of neural architectures (ILASH) for multi-task applications that reduces overall computation by sharing layers among tasks leading to reduced energy/emission overheads during inferencing.
- 2) Formulated a novel neural architecture search algorithm, appropriate for building ILASH models (ILASH-NAS), that uses AI to boost search efficiency while reducing energy/emission overheads.
- 3) Implemented a highly parameterized version of the ILASH-NAS that can generate layer-shared architectures for multi-task applications.
- 4) Evaluated ILASH-NAS and the generated ILASH models using standard datasets such as UTKFace, MTF, CelebA, and Taskonomy on different edge devices (NVIDIA Jetson AGX Orin, Orin Nano, Jetson Nano, and Raspberry Pi 4 Model B).

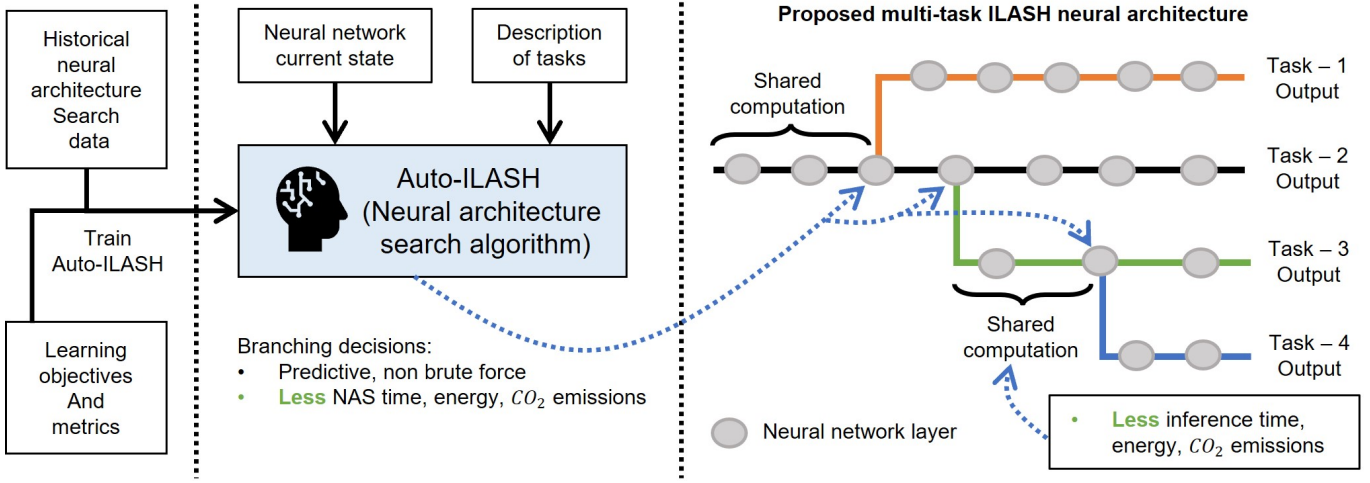


Fig. 1. Overview of the proposed ILASH architecture and the neural architecture search algorithm (ILASH-NAS).

II. BACKGROUND AND MOTIVATION

In this section, we will briefly describe multi-task learning and neural architecture search (NAS) algorithms.

TABLE I
COMPARISON OF ENERGY CONSUMPTION AND CO₂ EMISSION AMONG STATE-OF-THE-ART NAS METHODS ON CIFAR-10 (*Not a Multitask application*).

Method	NVIDIA GPU	GPU Hours	kWh-PUE	CO ₂ emission (lbs)
AutoSNN [18]	RTX 2080 Ti	4.35×10^1	2.58×10^1	2.46×10^1
DCNN [19]	Tesla TitanXp	2.40×10^2	1.42×10^2	1.36×10^2
CNN-GA [20]	GTX 1080 Ti	8.40×10^2	4.98×10^2	4.75×10^2
NAS-RL [21]	Tesla K40	5.38×10^5	3.12×10^5	2.98×10^5
EAS [22]	GTX 1080	2.40×10^2	1.02×10^2	9.77×10^1
CGP-CNN [23]	GTX 1080	6.48×10^2	2.76×10^2	2.63×10^2
DARTS-PT [24]	GTX 1080 Ti	19.2	8.19	7.81
NAO [25]	Tesla V100	4.80×10^3	3.41×10^3	3.26×10^3
PNAS [26]	Tesla P100	5.40×10^3	3.20×10^3	3.05×10^3
NASNet [27]	Tesla P100	4.80×10^4	2.84×10^4	2.71×10^4
Hierarchical-EAS [28]	Tesla P100	7.20×10^3	4.27×10^3	4.07×10^3

A. Traditional Neural Architecture Search

Neural Architecture Search (NAS) algorithms are widely used for finding optimal neural architectures for a given application. Recently, Spiking Neural Networks (SNNs) have garnered significant attention, with studies like AutoSNN by Na *et al.* [18], which explore hyperparameters within a pre-established search space. SeqNAS was introduced by Udovichenko *et al.* [35] to classify event sequences, using Bayesian optimization in conjunction with multi-head self-attention convolutional neural networks. Meanwhile, Wang *et al.* proposed DARTS-PT [24], a perturbation-based approach that improves generalization through the evaluation of supernet operation. Even with all these innovations, state-of-the-art (SOTA) NAS algorithms are still iterative in nature, resource-intensive [36] and time-consuming (see Table II and Table I). Moreover standard NAS techniques are not designed for building multi-task neural networks and hence a direct

comparison with ILASH is not possible. Table I shows the statistics of GPU hours, energy consumption, and equivalent CO₂ emission associated with different NAS methods for the CIFAR10 dataset. Energy consumption and CO₂ emission are calculated using [37]:

$$p_t = \frac{1.58t(p_c + p_r + gp_g)}{1000} \quad (1)$$

$$\text{CO}_2e = 0.954p_t \quad (2)$$

Here, t , p_c , p_r , and p_g denote the NAS runtime, average power consumed by the CPU, average power consumed by RAM, and average power consumed by GPU, respectively. ‘g’ stands for the total number of GPUs, and p_t is the power usage effectiveness (PUE) measured in kilowatt-hours (kWh). We assume the power usage of GTX 1080, GTX 1080 Ti, RTX 2080 Ti, and Tesla TitanXp to be 270 watt, 375 watt, 375 watt, and 375 watt respectively ($1.5 \times TDP$ [38]).

B. Multi-Task Learning and NAS

Multi-task learning involves training a single Artificial Intelligence (AI) model for performing multiple tasks. Multi-task learning is typically done to reduce weight size overhead for IoT devices. Recently, works such as Fast GraspNeXt [39], used a self-attention neural network model designed specifically for embedded multi-task learning. Li *et al.* [40] proposed a multi-task learning (MTL) strategy utilizing knowledge distillation to attain fair parameter sharing among multiple tasks. However, these techniques do not focus on building multi-task neural networks for reducing overall energy consumption and CO₂ emissions. Hence a direct comparison of ILASH with these techniques is not possible. However we qualitatively compare different NAS techniques with ILASH-NAS in Table II. Auto-Keras, a framework developed by Jin *et al.* in 2019 [31], implements some of the most well-known NAS algorithms such as Greedy, Random, and Bayesian in the context of multi-task learning (only publicly available framework). Hence, we compare ILASH with Auto-Keras algorithms to understand the effectiveness of ILASH (Sec IV).

TABLE II
QUALITATIVE COMPARISON BETWEEN ILASH-NAS AND OTHER NEURAL ARCHITECTURE SEARCH FRAMEWORKS.

Method	Efficiency based on GPU usage	Search Strategy	Multi-task Support			Single task Support	AI Driven
			Regression	Classification	2D Semantic		
NAS-RL [21]	Very Low	Cell-based	✗	✗	✗	✓	✗
EAS [22]	High	Transformation based	✗	✗	✗	✓	✗
Hierarchical-EAS [28]	Medium	Hierarchical	✗	✗	✗	✓	✗
AmoebaNet-A [29]	Low	Cell-based	✗	✗	✗	✓	✗
DARTS [30]	Medium	Cell-based	✗	✗	✗	✓	✗
PNAS [26]	Low	Cell-based	✗	✗	✗	✓	✗
AutoSNN [18]	Medium	Spiking Neural Network based	✗	✗	✗	✓	✗
Autokeras [31], [32]	Medium	Network Morphism	✓	✓	✗	✓	✗
CNN-GA [20]	Low	Mutation and Crossover	✗	✗	✗	✓	✗
DARTS-PT [24]	High	Gradient Stabilization	✗	✗	✗	✓	✗
GENIUS [33]	Medium	NAS-Bench	✗	✗	✗	✓	✓
DCNN [19]	Low	Mutation and Crossover	✗	✗	✗	✓	✗
CGP-CNN [23]	Low	Mutation based	✗	✗	✗	✓	✗
LeMo-NADe [34]	Medium	Open Search	✗	✗	✗	✓	✓
ILASH-Heu (Proposed)	Medium	Branching based	✓	✓	✓	✓	✗
ILASH-Pred (Proposed)	Very High	Branching based	✓	✓	✓	✓	✓

Algorithm 1: Heuristic Based Search: ILASH-Heu

```

Input:  $Model_{base}, Dataset, TaskInfoDict, ll, ul$ 
Output:  $ILASH\_Model, ILASH\_Dataset$ 
1  $ILASH\_Dataset = []$ ;  $ILASH\_Model \leftarrow \emptyset$ 
2 for  $taskIdx \leftarrow 0$  to  $len(TaskInfoDict)$  do
3   if  $taskIdx = 0$  then
4      $ILASH\_Model \leftarrow Model_{base}$ 
5      $Data \leftarrow Dataset[taskIdx]$ 
6      $ILASH\_Model.train(Data.tr)$ 
7   else
8      $Model \leftarrow ILASH\_Model$ 
9      $Data \leftarrow Dataset[taskIdx]$ ;  $BGN \leftarrow 0$ 
10    for  $idx, lr \in Model.layers()$  do
11      if  $(idx < ll)$  OR  $(idx > ul)$  then
12         $continue$ 
13       $temp\_model \leftarrow branch(Model, lr)$ 
14       $temp\_model.train(Data.tr)$ 
15       $GN \leftarrow Eval(temp\_model, Data.val)$ 
16      if  $GN > BGN$  then
17         $BGN \leftarrow GN$ 
18         $ILASH\_Model \leftarrow temp\_model$ 
19       $taskInfo \leftarrow TaskInfoDict[taskIdx]$ 
20       $layerInfo \leftarrow encode(idx, Model)$ 
21       $D \leftarrow [taskInfo, layerInfo, GN]$ 
22       $ILASH\_Dataset.append(D)$ 
23 return  $ILASH\_Model, ILASH\_Dataset$ 

```

III. METHODOLOGY

Next we formalize the ILASH architecture and the ILASH neural architecture search algorithms.

Algorithm 2: Layer Encoding: encode

```

Input:  $Model, idx$ 
Output:  $encodedLayer$ 
1  $temp \leftarrow \emptyset$ 
2 for  $i \leftarrow -1$  to 1 do
3    $lrType \leftarrow Model.layers[idx + i].type$ 
4   if  $lrType == Conv2D$  OR  $DepthwiseConv2D$  then
5      $lr \leftarrow Model.layers[idx + i]$ 
6      $temp.kernel_i \leftarrow lr.kernelSize$ 
7      $temp.pad_i \leftarrow (1 \text{ if } lr.pad == valid \text{ else } 0)$ 
8      $temp.stride_i \leftarrow lr.strideSize$ 
9   else
10     $temp.kernel_i \leftarrow -1$ 
11     $temp.pad_i \leftarrow -1$ 
12     $temp.stride_i \leftarrow -1$ 
13  $encodedLayer \leftarrow temp$ 
14 return  $encodedLayer$ 

```

A. ILASH: Layer Shared Architecture

Fig. 1 shows the overview of our proposed ILASH architecture. The proposed approach is a hybrid between the hard-layer-sharing approaches and the non-sharing approach (i.e. separate models for each task). Assume that a system needs to perform p tasks (T_1, T_2, \dots , and T_P) such that $T_1 = \{l_1^1, l_2^1, l_3^1, \dots, l_{n_1}^1\}$, $T_2 = \{l_1^2, l_2^2, l_3^2, \dots, l_{n_2}^2\}$, and $T_P = \{l_1^p, l_2^p, l_3^p, \dots, l_{n_p}^p\}$. Here l_x^y is the x^{th} layer of the y^{th} task. Also P is a set of numbers $\{1, 2, \dots, p\}$. The differences between these strategies are as follows.

- 1) **No Sharing:** For this, $\forall x \in T_a, x \notin \bigcup_{i \in P-a} T_i$. This implies that, no two layers are the same among all the

tasks (i.e. completely separate models).

- 2) **Hard Layer Sharing:** In this case, $\forall y \in P$, l_1^y are the same, l_2^y are the same, and so on up to the second last layer. Only the last layer is different across all tasks.
- 3) **ILASH [Proposed]:** First we build $T_1 = \{l_1^1, l_2^1, \dots, l_{n1}^1\}$. Next we identify a layer $x \in T_1$ for branching out to support Task 2. This will lead to $T_2 = \{l_1^1, l_2^1, l_3^1, \dots, l_x^1, l_{x+1}^2, \dots, l_{n2}^2\}$. Note that we are reusing layers $\{l_1^1, l_2^1, l_3^1, \dots, l_x^1\}$ from Task 1 to support Task 2. Next to support Task 3, we pick a branching layer from the set of all unique layers ($T_1 \cup T_2$), connect extra layers from that branching point to support task 3, and reuse all prior layers from that point for task 3. This process continues until all tasks are supported. Fig. 1 provides a visual representation of the proposed network architectures. The ILASH architecture is a hybrid between ‘No Sharing’ and ‘Hard Layer Sharing’.

For ILASH, the branching process determines the efficacy for the overall network and to efficiently handle this process, we propose two mechanisms for ILASH neural architecture search (ILASH-NAS) described next: (1) A heuristics approach and (2) A predictive approach using AI/ML.

B. Heuristic Based ILASH-NAS

Our initial goal is to build a heuristic-driven neural network search algorithm for layer-shared models that will allow us to capture the necessary information (dataset) required to build an AI-guided version of the NAS framework. This NAS algorithm (ILASH-Heu) is described using Algorithm 1 and Algorithm 2.

The inputs of Algorithm 1 are as follows:

- $Model_{base}$: This is the neural network model upon which all subsequent adaptations and refinements will be made. It acts as the model for Task-1.
- $Dataset$: The dataset is the collection of data points used for training the model (for all tasks). It includes input data and corresponding target labels, providing the necessary information for the model to learn and adapt.
- $TaskInfoDict$: This dictionary contains information about each task such as input shape of the data, shape of the expected output, choice of loss function, metrics used for evaluating the model’s performance, and the hyperparameters to fine-tune the model during training.
- Upper limit (ul) and Lower limit (ll): The lower and upper limits determine the layer position boundaries between which branching is allowed.

In Algorithm 1, ILASH-Heu initiates the process by training the base model on the task-1 dataset (lines 3 to 6). From the second task onward, the algorithm attempts to branch off from all layers having a depth higher than ll and lower than ul in the existing network (line 11). Based a branching choice/location (lr) a temporary network (temp_model) is created by replicating the base model layers from the branching location (lr) to the 2nd last layer. An output layer based on the number of outputs of the task is added at the end with an appropriate activation function depending on the type of task (classification, regression, etc.). In lines 14 and 15, this temporary network (temp_model) is then trained and evaluated

Algorithm 3: Predictive Based Search: ILASH-Pred

Input: $Model_{base}, Auto_ILASH, Dataset, TaskInfo, ll, ul$
Output: $BestModel$

```

1  $ILASH\_Model \leftarrow \emptyset$ 
2 for  $T\_idx \leftarrow 0$  to  $len(TaskInfo)$  do
3   if  $T\_idx = 0$  then
4      $ILASH\_Model \leftarrow Model_{base}$ 
5   else
6      $BGN \leftarrow 0; bestBr \leftarrow \emptyset$ 
7     for  $idx, lr \in ILASH\_Model.layers()$  do
8       if  $(idx < ll)$  OR  $(idx > ul)$  then
9          $continue$ 
10       $data \leftarrow [TaskInfo[T\_idx], lr.encode()]$ 
11       $GN \leftarrow Auto\_ILASH.predict(data)$ 
12      if  $GN > BGN$  then
13         $BGN \leftarrow GN$ 
14         $bestBr \leftarrow lr$ 
15       $ILASH\_Model.branch(bestBr)$ 
16  $ILASH\_Model.train(Dataset.tr)$ 
17 return  $ILASH\_Model$ 

```

for obtaining its Goodness Metric (GN) using Eqn 3. The model ($ILASH_Model$) corresponding to the best branching location (lr) and the best Goodness Metric value (BGN) are tracked in lines 16-18. Inside $ILASH_Dataset$ (line 22), we track the Goodness Metric (GN) value associated with each branching decision along with information of the task being handle and an encoding computed based on the layer from which branching was done. Algorithm 1 returns a layer-shared model for all the given tasks in line 23. Algorithm 2 shows the overall layer encoding process which takes the $Model$ and branching layer index (idx) as input and generates an encoding for representing this branching layer. The encoding process captures the information about the branching layer and its surrounding layers as a vector representation. This encoding is required later for the predictive ILASH-NAS process (discussed in Sec. III-C).

To address the concern regarding how energy consumption and carbon emissions are considered (or the lack thereof) in the NAS process, we propose a metric called Goodness (GN). This metric is calculated using the following equation:

$$GN = acc \times (1 - G_{th}) + \left(\frac{lr_{index}}{lr_{total}} \right) \times G_{th} \quad (3)$$

Here, acc represents the validation accuracy of the model, while the green threshold (G_{th}) is a user-controlled parameter that balances accuracy and network efficiency. The term $\frac{lr_{index}}{lr_{total}}$ indicates the relative position of the layer within the total number of layers, with G_{th} serving as a weight to reflect the preference between accuracy and efficiency. By integrating lr_{index}/lr_{total} into the GN metric, we implicitly consider network efficiency, which is closely related to energy consumption and carbon emissions.

C. Predictive ILASH-NAS

The first step of the predictive ILASH_NAS is to train an AI model (*Auto – ILASH*) that can predict the goodness (GN) metric for a given branching choice during the ILASH model search. This prediction significantly speeds up the search process as demonstrated in the results section. We have experimented with different machine learning (ML) algorithms (to train the *Auto – ILASH* model) and we measure the performance of these ML algorithms using the following metrics.

- **Mean Absolute Error (MAE):** We can calculate MAE as follows:

$$\text{MAE} = \frac{1}{n} \sum_{i=1}^n |y_i - \hat{y}_i| \quad (4)$$

Here, n is the number of data points, y_i is the actual value, \hat{y}_i is the predicted value and $|y_i - \hat{y}_i|$ is the absolute error for each data point.

- **Mean Squared Error (MSE):** We calculate the MAE using the following equation:

$$\text{MSE} = \frac{1}{n} \sum_{i=1}^n (y_i - \hat{y}_i)^2 \quad (5)$$

Here, n is the number of data points, y_i is the actual value, \hat{y}_i is the predicted value and $(y_i - \hat{y}_i)^2$ is the squared error for each data point.

- **Root Mean Squared Error (RMSE):** The mean root squared error (RMSE) is calculate as follows:

$$\text{RMSE} = \sqrt{\frac{1}{n} \sum_{i=1}^n (y_i - \hat{y}_i)^2} \quad (6)$$

Here, n is the number of data points, y_i is the actual value, \hat{y}_i is the predicted value and $(y_i - \hat{y}_i)^2$ is the squared error for each data point.

- **R^2 Score:** We calculate the R^2 score using the following equation:

$$R^2 = 1 - \frac{\sum_{i=1}^n (y_i - \hat{y}_i)^2}{\sum_{i=1}^n (y_i - \bar{y})^2} \quad (7)$$

Here, n is the number of data points, y_i is the actual value, \hat{y}_i is the predicted value and \bar{y} is the mean of actual values.

Algorithm 3 shows the predictive ILASH-NAS process. Unlike ILASH-Heu, ILASH-Pred does not need to train the base model on the first given task. For each subsequent task, the Best Goodness (BGN) value is set to 0 and the best branching (*bestBr*) is set to empty in lines 6. In lines 7-13, we search for the best layer for branching and perform the branching process. Before predicting the Goodness (GN) of each layer we first check if the layer is in between *ul* and *ll*. In line 11, *Auto – ILASH* predicts the GN of the layer by using the encoding computed in line 10. In lines 12-14, we keep track of the best branching point (*bestBr*) and the best Goodness metric value (*BGN*). After checking all branching layer possibilities, ILASH-Pred builds a branched model for the task using *bestBr* (line 15). Based the branching

choice/location (*bestBr*) the branched model is created by replicating the base model layers from the branching location (*bestBr*) to the 2^{nd} last layer. An output layer based on the number of outputs of the task is added at the end with an appropriate activation function depending on the type of task (classification, regression, etc.). This process is continued for the remaining tasks. The final model (*ILASH_Model*) is trained on the training data for all tasks at the same time.

IV. EXPERIMENTAL SETUP AND DATA DESCRIPTION

Next we will discuss the experimental setup and the datasets.

A. Experimental Setup: Auto-ILASH

Auto-ILASH is the predictive component of the ILASH-Pred version of ILASH-NAS (see Algorithm 3. Auto-ILASH is an ML model and we have experimented with the following ML algorithms for realizing it (evaluation results in later section).

- **Random Forest (RF) Regressor:** Number of estimator = 100, criterion = ‘gini’, max_features = sqrt, max_features = 1.0, min_samples_split = 2.
- **Decision Tree (DT) Regressor:** Criterion = ‘squared_error’, splitter = ‘best’, min_sample_split = 2.
- **Linear Regressor:** For Linear Regressor, we used copy_X = True, fit_intercept = True.
- **Support Vector Regressor (SVR):** For SVR, we used kernel = ‘rbf’, gamma = ‘scale’, and epsilon = 0.1.
- **Gradient Boosting (GradBoost) Regressor:** For GradBoost Regressor, we used ‘squared_error’ loss, learning rate = 0.1, number of estimator = 100 and criterion = ‘friedman_mse’.

We use a leave-one-out strategy for creating the Auto-ILASH model. For example, when searching for the ILASH network for UTKFace, the Auto-ILASH model used by Algorithm 3 is trained on the two merged ILASH_Dataset obtained from the ILASH_Heu runs on MTFL and CelebA. Similarly for the Taskonomy Dataset, when we are searching for the model for Taskonomy-1, we train the Auto-ILASH model on the two merged ILASH_Dataset obtained from the ILASH_Heu runs on Taskonomy-2 and Taskonomy-3. When training the Auto-ILASH model, we split the data in a 7:3 ratio for training and validation purposes respectively.

B. Experimental Setup: Edge Devices

As target edge devices (for measuring inference-time efficiency) we have used NVIDIA Jetson AGX Orin, Orin Nano, Jetson Nano, and Raspberry Pi 4 Model B. For these devices, we measure the power consumption using plug-in monitors and calculate the equivalent energy consumption (KWh-PUE) and CO₂ emissions with the help of eqn. 1 and 2. Our edge computing setup is shown in Fig. 2).

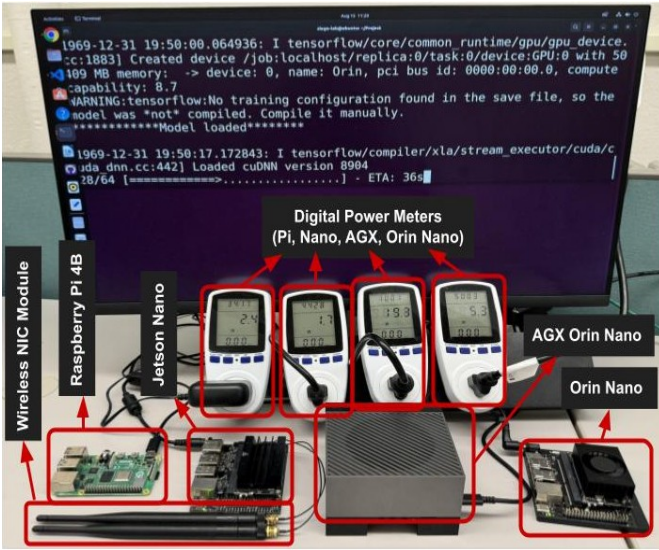


Fig. 2. Inferencing setup using target edge devices.

TABLE III
EFFICACY OF DIFFERENT MACHINE LEARNING ALGORITHMS FOR BUILDING THE ILASH-NAS BRANCHING MODEL. RF = RANDOM FOREST, DT = DECISION TREE, LINEAR = LINEAR REGRESSION, SVR = SUPPORT VECTOR REGRESSION, AND GRADBOOST = GRADIENT BOOSTING REGRESSOR.

Model	MAE	MSE	RMSE	R^2
RF	0.033	0.002	0.045	0.971
DT	0.027	0.002	0.044	0.973
Linear	0.054	0.004	0.063	0.942
SVR	0.113	0.020	0.142	0.701
GradBoost	0.040	0.002	0.049	0.965

C. Experimental Setup: Task Models

For both process (ILASH-Heu, ILASH-Pred), when training the ILASH task models, we use Adam optimizer with a learning rate of 1×10^{-3} , batch size of 32, and 50 epochs. In the pre-processing stage, we resize all images to (128×128) and split them up into training, validation and testing sets with a ratio of 70%, 10% and 20% respectively. For searching with AutoKeras, we use a *max_trial* of 20 for all methods (Greedy, Random and Bayesian). All neural search and training are performed on the following setup: {AMD EPYC 2 Rome CPU, Nvidia A100 GPU 40 GB, 128 GB RAM}. To measure the power draw of GPU and CPU during network search/training, we used pyJoules [41] (Python Library). We used eqn. 1 and 2 to calculate the power consumption and equivalent CO_2 emission for all experiments. We use MobileNet [42] as the base model (*Model_base* in Algo. 1 and Algo. 3) for classification/regression tasks (UTKFace, MTFI, and CelebA Datasets). We use MobileNet as the encoder, followed by six Conv2DTranspose layers with channel sizes of 512, 256, 128, 64, 32, and 1 (with ReLU activation) acting as the decoder as the base model (*Model_base* in Algo. 1 and Algo. 3) for 2D semantic tasks (Taskonomy Datasets).

D. Data Description

In this study, we considered three different datasets (a) UTKFace [14], (b) MTFI [15] and (c) CelebA [16] for image classification and regression tasks, and the Taskonomy [17] dataset for 2D semantic tasks.

1) **UTKFace**: The UTKFace dataset is a widely used and publicly available collection of facial images that is often used in the field of computer vision and machine learning research. The dataset consists of more than 20,000 facial images representing different individuals. Each image is annotated with the individual's gender (C_1), race (C_2), and age (R_1) that are used as labels for our multi-task applications. The order in which each of these tasks are presented to the ILASH-NAS algorithms can affect the overall performance hence we report the ILSH_Pred results for two task orders: (1) C_1, C_2, R_1 represented by ILSH_Pred-1 in the results; (2) C_2, R_1, C_1 represented by ILSH_Pred-2 in the results.

2) **MTFI**: The multi-task facial landmark (MTFI) dataset is a collection of facial images that have been annotated with multiple sets of facial landmarks/attributes. These landmarks are defined as crucial points or coordinates on the face that correspond to distinct facial features, including but not limited to the eyes, nose, and mouth. The dataset includes attributes (used as multi-task labels) such as gender (C_1), smiling expression (C_2), glasses-wearing (C_3), and head pose (C_4). The order in which each of these tasks are presented to the ILASH-NAS algorithms can affect the overall performance hence we report the ILSH_Pred results for two task orders: (1) C_1, C_2, C_3, C_4 represented by ILSH_Pred-1 in the results; (2) C_3, C_4, C_1, C_2 represented by ILSH_Pred-2.

3) **CelebA**: CelebA is widely used for face recognition, detection, and facial landmark prediction. We consider 5 attributes i.e., Gender (C_1), Hair color (C_2), Hair style (C_3), Smiling (C_4) and Nose (C_5) for our multi-task classification application. We randomly choose 20K images for our experiments. The order in which each of these tasks are presented to the ILASH-NAS algorithms can affect the overall performance hence we report the ILSH_Pred results for two task orders: (1) C_1, C_2, C_3, C_4, C_5 represented by ILSH_Pred-1 in the results; (2) C_4, C_2, C_5, C_3, C_1 represented by ILSH_Pred-2.

4) **Taskonomy**: Taskonomy is a widely used dataset for 2D semantic tasks. This dataset consists of 4.6 million indoor scenes from 537 buildings. It has 4 different versions: Tiny, Medium, Full and Full+ containing indoor images from 35, 138, 482 and 537 buildings respectively. In this study, we use data from the tiny category to perform 2D edge texture (T_1), surface normal (T_2), and reshading (T_3) tasks. We divide the tiny taskonomy dataset into three parts based on unique buildings and every part is considered as a separate dataset to evaluate our approach. The order in which each of these tasks are presented to the ILASH-NAS algorithms can affect the overall performance hence we report the ILSH_Pred results for two task orders: (1) T_1, T_2, T_3 represented by ILSH_Pred-1 in the results; (2) T_2, T_3, T_1 represented by ILSH_Pred-2 in the results.

V. EXPERIMENTAL RESULTS AND ANALYSIS

In this section, we will discuss the experimental results.

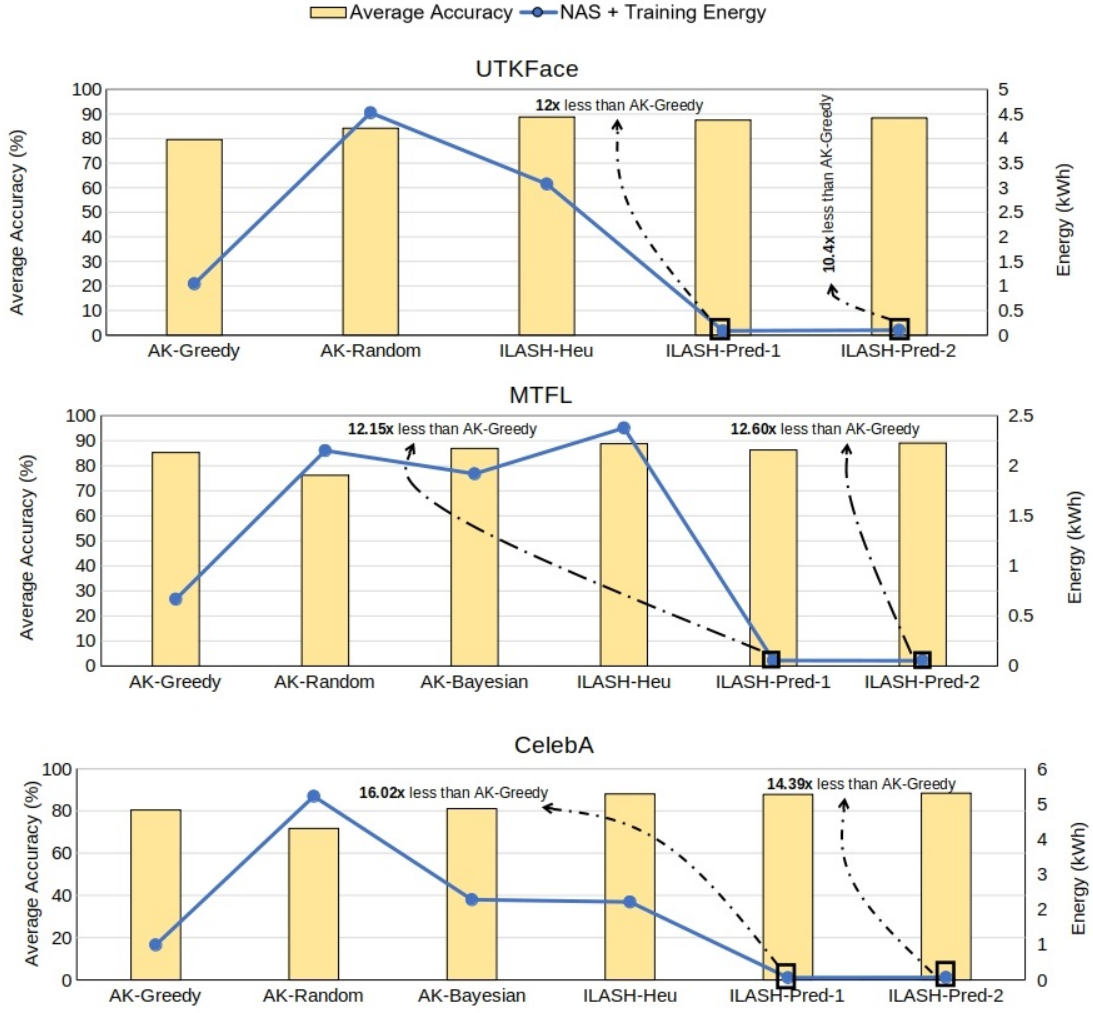


Fig. 3. **UTKFace, MTFL, and CelebA Datasets:** Neural search efficiency and model accuracy comparison between ILASH and other state-of-the-art multitask NAS algorithms.

TABLE IV

UTKFACE, MTFL, AND CELEBA DATASETS: RESULTS SHOWING INFERRING EFFICACY OF ILASH AND AUTOKERAS (AK) ON NVIDIA JETSON AGX ORIN, ORIN NANO, JETSON NANO, AND RASPBERRY PI.

Datasets	Method	Inference in Jetson AGX Nano (per image)			Inference in Jetson Orin Nano (per image)			Inference in Jetson Nano (per image)			Inference in Raspberry Pi (per image)		
		KWh-PUE ($\times 10^{-8}$)	CO ₂ Emission ($\times 10^{-8}$ lbs)	FPS	KWh-PUE ($\times 10^{-8}$)	CO ₂ Emission ($\times 10^{-8}$ lbs)	FPS	KWh-PUE ($\times 10^{-6}$)	CO ₂ Emission ($\times 10^{-7}$ lbs)	FPS	KWh-PUE ($\times 10^{-7}$)	CO ₂ Emission ($\times 10^{-7}$ lbs)	FPS
UTKFace [14]	AK-Greedy	3.45	3.29	131.33	2.95	2.81	112.26	1.16	1.11	15.95	2.31	2.20	5.31
	AK-Random	1.33	1.27	161.46	2.05	1.95	151.86	1.17	1.06	18.56	2.11	2.02	6.43
	ILASH-Heu	1.0	0.957	351.69	1.58	1.46	288.56	0.597	0.569	58.07	0.804	0.767	17.53
	ILASH-Pred-1	1.06	1.01	357.02	1.25	1.19	296.57	0.564	0.538	56.18	0.827	0.789	16.99
	ILASH-Pred-2	1.05	1.01	349.85	1.01	0.965	291.62	0.481	0.458	55.48	0.774	0.738	18.45
MTFL [15]	AK-Greedy	5.37	5.13	92.17	4.63	4.42	83.56	5.18	4.94	10.56	5.24	5.0	2.59
	AK-Bayesian	6.49	6.19	66.91	6.02	5.74	57.62	5.24	5.0	11.48	4.99	4.76	2.55
	AK-Random	2.34	2.23	145.16	2.45	2.34	129.78	4.32	4.12	21.56	2.33	2.23	7.12
	ILASH-Heu	1.04	0.993	256.18	0.107	0.102	221.56	0.682	0.651	52.12	0.802	0.766	17.97
	ILASH-Pred-1	0.830	0.791	265.68	0.937	0.894	228.04	0.689	0.657	54.15	0.649	0.619	23.71
ILASH-Pred-2	0.913	0.871	267.66	0.935	0.892	184.7	0.715	0.682	53.87	0.576	0.550	24.15	
CelebA [16]	AK-Greedy	2.04	1.94	214.6	2.44	2.33	186.21	1.90	1.81	15.86	2.37	2.27	6.47
	AK-Bayesian	5.90	5.62	56.63	6.42	6.13	53.55	2.11	2.01	9.4	7.17	6.84	2.02
	AK-Random	5.49	5.23	56.7	6.48	6.18	52.22	1.85	1.76	11.5	7.15	6.83	2.03
	ILASH-Heu	8.31	0.793	337.76	0.814	0.776	268.79	0.579	0.553	59.06	0.599	0.571	23.54
	ILASH-Pred-1	0.735	0.701	340.36	0.806	0.769	275.56	0.543	0.518	58.14	0.412	0.393	23.56
ILASH-Pred-2	0.836	0.798	336.48	0.681	0.650	296.42	0.511	0.488	62.15	3.88	3.70	25.46	

TABLE V
TASKONOMY DATASET: RESULTS SHOWING INFERENCING EFFICACY OF ILASH ON NVIDIA JETSON AGX ORIN, ORIN NANO, JETSON NANO, AND RASPBERRY PI.

Datasets	Method	Inference in Jetson AGX Nano (per image)			Inference in Jetson Orin Nano (per image)			Inference in Jetson Nano (per image)			Inference in Raspberry Pi (per image)		
		KWh-PUE ($\times 10^{-8}$)	CO ₂ Emission ($\times 10^{-8}$ lbs)	FPS	KWh-PUE ($\times 10^{-8}$)	CO ₂ Emission ($\times 10^{-8}$ lbs)	FPS	KWh-PUE ($\times 10^{-6}$)	CO ₂ Emission ($\times 10^{-7}$ lbs)	FPS	KWh-PUE ($\times 10^{-7}$)	CO ₂ Emission ($\times 10^{-7}$ lbs)	FPS
1	ILASH-Heu	1.0	0.957	351.69	1.58	1.46	288.56	0.597	0.569	58.07	0.804	0.767	17.53
	ILASH-Pred-1	1.06	1.01	357.02	1.25	1.19	296.57	0.564	0.538	56.18	0.827	0.789	16.99
	ILASH-Pred-2	1.05	1.01	349.85	1.01	0.965	291.62	0.481	0.458	55.48	0.774	0.738	18.45
2	ILASH-Heu	1.04	0.993	256.18	0.107	0.102	221.56	0.682	0.651	52.12	0.802	0.766	17.97
	ILASH-Pred-1	0.830	0.791	265.68	0.937	0.894	228.04	0.689	0.657	54.15	0.649	0.619	23.71
	ILASH-Pred-2	0.913	0.871	267.66	0.935	0.892	184.7	0.715	0.682	53.87	0.576	0.550	24.15
3	ILASH-Heu	8.31	0.793	337.76	0.814	0.776	268.79	0.579	0.553	59.06	0.599	0.571	23.54
	ILASH-Pred-1	0.735	0.701	340.36	0.806	0.769	275.56	0.543	0.518	58.14	0.412	0.393	23.56
	ILASH-Pred-2	0.836	0.798	336.48	0.681	0.650	296.42	0.511	0.488	62.15	3.88	3.70	25.46

TABLE VI

TASKONOMY DATASET: NEURAL SEARCH EFFICIENCY AND MODEL MAE (PERFORMANCE) COMPARISON BETWEEN DIFFERENT ILASH SETTINGS.

Datasets	Method	Average MAE	NAS and Final Training		
			Runtime (Hrs)	kWh-PUE	CO ₂ emission (lbs)
1	ILASH-Heu	0.0821	60.2	6.34	6.05
	ILASH-Pred-1	0.0749	1.58	0.287	0.273
	ILASH-Pred-2	0.0756	1.44	0.247	0.245
2	ILASH-Heu	0.0798	48.73	5.73	5.44
	ILASH-Pred-1	0.0787	1.30	0.239	0.228
	ILASH-Pred-2	0.0775	1.18	0.183	0.174
3	ILASH-Heu	0.0810	53.6	5.78	5.49
	ILASH-Pred-1	0.0785	1.48	0.262	0.249
	ILASH-Pred-2	0.0795	1.39	0.240	0.228

A. Auto-ILASH Model Selection

The Auto-ILASH model used in Algorithm 3 (ILASH-Pred, the predictive version of ILASH-NAS) is trained on the data, ILASH_Dataset, obtained from Algorithm 1 runs (ILASH-Heu, the heuristics version of ILASH-NAS). We have experimented with different machine learning (ML) algorithms for creating the most optimal Auto-ILASH model. Table III shows these experimental results. Among the five ML model, Decision Tree performs better in terms of MAE, MSE, RMSE and R^2 score. Based on this evaluation we decided to use the Decision Tree algorithm for building the final Auto-ILASH model.

B. Evaluation on the UTKFace, MTFI, and CelebA Datasets

In Figure 3, we compare the final model accuracy (across all the tasks for the given dataset) and the energy utilization for neural architecture search (+training). We see that the overall final accuracy of the system remains mostly stable across all the techniques, however, our proposed ILASH-Pred technique (for both task ordering) is extremely energy efficient. The order in which each of these tasks are presented to the ILASH-NAS algorithms can affect the overall performance hence we report the ILSH_Pred results for two task orders (more details in Section IV). Here AK-Greedy refers to AutoKeras with ‘greedy’ tuner, AK-Random refers to AutoKeras with ‘random’ tuner, and AK-Bayesian refers to AutoKeras with

‘bayesian’ tuner. For more details about AutoKeras please refer to [31], [32]. We see very similar trend across all the three datasets MTFI, CelebA, and UTKFace. AK-Greedy is the least energy intensive approach among all AutoKeras techniques. Even then ILSH_Pred is 10-16 times more efficient. This is made possible due to the Auto_ILASH model making the branching decisions with very little delay. ILASH_Heu is not the most optimal approach and should be only used for creating the initial dataset necessary to build the Auto_ILASH model for ILASH_Pred.

Next we evaluate the efficacy (during inferencing/deployment) of the final searched models obtained via different variants of AutoKeras and ILASH-NAS for the UTKFace, MTFI, and CelebA Datasets (see Table IV). We use four different edge devices (NVIDIA Jetson AGX Orin, Orin Nano, Jetson Nano, and Raspberry Pi 4 Model B) to extensively test the efficacy of the final model. These results conclusively demonstrates that both ILASH_Heu and ILASH_Pred leads to more optimal neural networks for edge devices in terms of energy consumption (KWh-PUE), CO₂ emission, and frames processed per second (FPS).

C. Evaluation on the Taskonomy Dataset

Next we perform a separate set of experiments to estimate the efficacy of ILASH-NAS (both ILASH_Heu and ILASH_Pred) for building multi-task networks to support 2D semantics tasks (2D edge texture, surface normal, and reshading). More details about the dataset used can be found in Section IV-D. Table VI shows the corresponding experimental results. Note that, we are unable to compare our results with AutoKeras because it (AutoKeras) does not support 2D semantics tasks. Hence, to the best of our knowledge, ILASH-NAS is the only multi-task neural architecture search framework that supports 2D semantics tasks. In Table VI we observe that ILASH_Pred (utilizing the Auto-ILASH ML Model) is approximately 38 times faster than ILASH-Heu method during the network search process resulting in nearly 22 times more energy efficiency (without much loss in final model MAE/performance). Next we evaluate the efficacy (during inferencing/deployment) of the final searched models

obtained via different variants of ILASH-NAS for the Taskonomy Dataset (see Table V). ILASH-Pred shows promising performance in every aspects.

VI. CONCLUSION

AI will play a major role in every aspect of human life in the near future. However, to make the pervasive AI dream a reality, we must analyze and mitigate its impact on energy utilization and the environment. In this work, we have presented a layer-shared neural architecture and a predictive NAS algorithm that leads to a dramatic reduction in energy/emission overheads (during architecture search & inferencing) for multi-task applications. Future works will explore AI-guided NAS for more complex applications and neural network topology.

REFERENCES

- [1] S. Rai, "Ai market will surge to near \$1 trillion by 2027, bain says." Accessed: 2024-11-06.
- [2] M. Weber, T. Weiss, F. Gechter, and R. Kriesten, "Approach for improved development of advanced driver assistance systems for future smart mobility concepts," *Autonomous Intelligent Systems*, vol. 3, no. 1, p. 2, 2023.
- [3] J. Dong, S. Chen, M. Miralinaghi, T. Chen, P. Li, and S. Labi, "Why did the ai make that decision? towards an explainable artificial intelligence (xai) for autonomous driving systems," *Transportation research part C: emerging technologies*, vol. 156, p. 104358, 2023.
- [4] M. Xu, D. Niyato, J. Chen, H. Zhang, J. Kang, Z. Xiong, S. Mao, and Z. Han, "Generative ai-empowered simulation for autonomous driving in vehicular mixed reality metaverses," *IEEE Journal of Selected Topics in Signal Processing*, 2023.
- [5] P. Ponce, B. Anthony, R. Bradley, J. Maldonado-Romo, J. I. Méndez, L. Montesinos, and A. Molina, "Developing a virtual reality and ai-based framework for advanced digital manufacturing and nearshoring opportunities in mexico," *Scientific Reports*, vol. 14, no. 1, p. 11214, 2024.
- [6] A. Kusiak, "Federated explainable artificial intelligence (fxai): a digital manufacturing perspective," *International Journal of Production Research*, vol. 62, no. 1-2, pp. 171–182, 2024.
- [7] M. Chua, D. Kim, J. Choi, N. G. Lee, V. Deshpande, J. Schwab, M. H. Lev, R. G. Gonzalez, M. S. Gee, and S. Do, "Tackling prediction uncertainty in machine learning for healthcare," *Nature Biomedical Engineering*, vol. 7, no. 6, pp. 711–718, 2023.
- [8] R. Bhardwaj and I. Tripathi, "An enhanced reversible data hiding algorithm using deep neural network for e-healthcare," *Journal of Ambient Intelligence and Humanized Computing*, vol. 14, no. 8, pp. 10567–10585, 2023.
- [9] S. Nandy, M. Adhikari, V. Balasubramanian, V. G. Menon, X. Li, and M. Zakarya, "An intelligent heart disease prediction system based on swarm-artificial neural network," *Neural Computing and Applications*, vol. 35, no. 20, pp. 14723–14737, 2023.
- [10] Q. Wang, X. Ji, and N. Zhao, "Embracing the power of ai in retail platform operations: Considering the showrooming effect and consumer returns," *Transportation Research Part E: Logistics and Transportation Review*, vol. 182, p. 103409, 2024.
- [11] M. S. Vhatkar, R. D. Raut, R. Gokhale, M. Kumar, M. Akarte, and S. Ghoshal, "Leveraging digital technology in retailing business: Unboxing synergy between omnichannel retail adoption and sustainable retail performance," *Journal of Retailing and Consumer Services*, vol. 81, p. 104047, 2024.
- [12] E. Strubell, A. Ganesh, and A. McCallum, "Energy and policy considerations for deep learning in nlp," *arXiv:1906.02243*, 2019.
- [13] IoT Analytics, "State of IoT—spring 2023." <https://iot-analytics.com/product/state-of-iot-spring-2023/>, 2023. Accessed: November 6, 2024.
- [14] A. Das, A. Dantcheva, and F. Bremond, "Mitigating bias in gender, age and ethnicity classification: a multi-task convolution neural network approach," in *Proceedings of the european conference on computer vision (eccv) workshops*, pp. 0–0, 2018.
- [15] Z. Zhang, P. Luo, C. C. Loy, and X. Tang, "Facial landmark detection by deep multi-task learning," in *Computer Vision—ECCV 2014: 13th European Conference, Zurich, Switzerland, September 6–12, 2014, Proceedings, Part VI 13*, pp. 94–108, Springer, 2014.
- [16] Z. Liu, P. Luo, X. Wang, and X. Tang, "Large-scale celebfaces attributes (celeba) dataset," *Retrieved Aug*, vol. 15, 2018.
- [17] A. R. Zamir *et al.*, "Taskonomy: Disentangling task transfer learning," in *Proceedings of the IEEE conference on computer vision and pattern recognition*, pp. 3712–3722, 2018.
- [18] B. Na, J. Mok, S. Park, D. Lee, H. Choe, and S. Yoon, "Autosnn: Towards energy-efficient spiking neural networks," in *International Conference on Machine Learning*, pp. 16253–16269, PMLR, 2022.
- [19] B. Ma *et al.*, "Autonomous deep learning: A genetic dcnn designer for image classification," vol. 379, pp. 152–161, 2020.
- [20] Y. Sun *et al.*, "Automatically designing cnn architectures using the genetic algorithm for image classification," *IEEE transactions on cybernetics*, vol. 50, no. 9, pp. 3840–3854, 2020.
- [21] B. Zoph and Q. V. Le, "Neural architecture search with reinforcement learning," *arXiv preprint arXiv:1611.01578*, 2016.
- [22] H. Cai, T. Chen, W. Zhang, Y. Yu, and J. Wang, "Efficient architecture search by network transformation," in *Proceedings of the AAAI Conference on Artificial Intelligence*, vol. 32, 2018.
- [23] M. Suganuma, M. Kobayashi, S. Shirakawa, and T. Nagao, "Evolution of deep convolutional neural networks using cartesian genetic programming," *Evolutionary computation*, vol. 28, no. 1, pp. 141–163, 2020.
- [24] R. Wang, M. Cheng, X. Chen, X. Tang, and C.-J. Hsieh, "Re-thinking architecture selection in differentiable nas," *arXiv preprint arXiv:2108.04392*, 2021.
- [25] R. Luo *et al.*, "Neural architecture optimization," *Advances in neural information processing systems*, vol. 31, 2018.
- [26] C. Liu *et al.*, "Progressive neural architecture search," in *Proceedings of the European conference on computer vision (ECCV)*, pp. 19–34, 2018.
- [27] B. Zoph *et al.*, "Learning transferable architectures for scalable image recognition," in *Proceedings of the IEEE conference on computer vision and pattern recognition*, pp. 8697–8710, 2018.
- [28] H. Liu, K. Simonyan, O. Vinyals, C. Fernando, and K. Kavukcuoglu, "Hierarchical representations for efficient architecture search," *arXiv preprint arXiv:1711.00436*, 2017.
- [29] E. Real, A. Aggarwal, Y. Huang, and Q. V. Le, "Regularized evolution for image classifier architecture search," in *Proceedings of AAAI conference on artificial intelligence*, vol. 33, pp. 4780–4789, 2019.
- [30] H. Liu, K. Simonyan, and Y. Yang, "Darts: Differentiable architecture search," *arXiv preprint arXiv:1806.09055*, 2018.
- [31] H. Jin, Q. Song, and X. Hu, "Auto-keras: An efficient neural architecture search system," in *ACM SIGKDD international conference on knowledge discovery & data mining*, pp. 1946–1956, 2019.
- [32] H. Jin, F. Chollet, Q. Song, and X. Hu, "Autokeras: An automl library for deep learning," *Journal of Machine Learning Research*, vol. 24, no. 6, pp. 1–6, 2023.
- [33] M. Zheng, X. Su, S. You, F. Wang, C. Qian, C. Xu, and S. Albanie, "Can gpt-4 perform neural architecture search?," *arXiv preprint arXiv:2304.10970*, 2023.
- [34] M. H. Rahman and P. Chakraborty, "Lemo-nade: Multi-parameter neural architecture discovery with llms," *arXiv preprint arXiv:2402.18443*, 2024.
- [35] I. Udovichenko *et al.*, "Seqnas: Neural architecture search for event sequence classification," *IEEE Access*, 2024.
- [36] M. M. Rizvee, M. H. Rahman, P. Chakraborty, and S. Shomaji, "Understanding the innovations required for a green & secure artificial intelligence paradigm," in *2023 IEEE 16th Dallas Circuits and Systems Conference (DCAS)*, pp. 1–6, IEEE, 2023.
- [37] E. Strubell, A. Ganesh, and A. McCallum, "Energy and policy considerations for modern deep learning research," in *Proceedings of the AAAI conference on artificial intelligence*, vol. 34, pp. 13693–13696, 2020.
- [38] I. Cutress, "Why intel processors draw more power than expected: Tdp and turbo explained," 2022.
- [39] A. Wong *et al.*, "Fast graspnext: A fast self-attention neural network architecture for multi-task learning in computer vision tasks for robotic grasping on the edge," in *CVPR*, pp. 2292–2296, 2023.
- [40] W.-H. Li and H. Bilen, "Knowledge distillation for multi-task learning," in *Computer Vision—ECCV 2020 Workshops: Glasgow, UK, August 23–28, 2020, Proceedings, Part VI 16*, pp. 163–176, Springer, 2020.
- [41] powerapi ng, "PyJoules: Python-based energy measurement library for various domains including NVIDIA GPUs." <https://github.com/powerapi-ng/PyJoules>, 2024. Accessed: 2024-01-10.
- [42] A. G. Howard *et al.*, "Mobilenets: Efficient convolutional neural networks for mobile vision applications," *arXiv:1704.04861*, 2017.